Impact of Cylinder Deactivation Strategies on Three-way Catalyst Performance in High Efficiency Low Emissions Engines

Brinklow, George; Herreros, Martin; Zeraati Rezaei, Soheil; Doustdar, Omid; Tsolakis, Athanasios; Millington, Paul; Kolpin, Amy

DOI:
10.1016/j.ceja.2023.100481

Chemical Engineering Journal Advances 14 (2023) 100481

Contents lists available at ScienceDirect

Chemical Engineering Journal Advances

journal homepage: www.sciencedirect.com/journal/chemical-engineering-journal-advances

Impact of Cylinder Deactivation Strategies on Three-way Catalyst Performance in High Efficiency Low Emissions Engines

George Brinklow [a,*], Jose Martin Herreros [a], Soheil Zeraati Rezaei [a], Omid Doustdar [a], Athanasios Tsolakis [a], Paul Millington [b], Amy Kolpin [b]

[a] Department of Mechanical Engineering, University of Birmingham, Edgbaston, B15 2TT, UK
[b] Johnson Matthey Technology Centre, Blount's Court, Sonning Common, Reading, RG4 9NH, UK

ARTICLE INFO

Keywords:
Automotive Three-Way Catalyst
Hybrid Vehicles
Euro VII Emissions
Pollution
Thermal Management

ABSTRACT

Reduction of CO2 emissions is a prevalent subject in the transportation sector. Cylinder deactivation (CDA) provides a method to reduce CO2 emissions at part load. However, there is little consideration of how these strategies affect catalyst performance.

Effects of two CDA strategies on catalyst performance were studied. The first strategy of open-loop lambda control CDA improved catalyst CO conversion to 100 % and prevented NH3 formation over the catalyst. There was a NOX penalty if the duration exceeded 5 seconds. The closed-loop CDA strategy increased catalyst temperature by 300°C for durations of 60 seconds.

Open-loop CDA can prevent NH3 formation and improve CO conversion. Closed-loop CDA strategy has potential to increase catalyst temperature and be effective at reducing light-off during cold starts without additional hardware. This gives the strategy an advantage over more complex heating options. Both strategies provide opportunities to help meet current and future emission regulations.

1. Introduction

The automotive sector is undergoing developments to achieve the ambitious CO_2 emission targets set globally. Electrification is being cited as the development to alleviate the contribution of the automotive sector to global CO_2 emissions. However, more than 97 % of new cars sold in 2019 utilised an internal combustion engine [1]. Furthermore, it is projected that internal combustion engine (ICE) powered vehicles (including hybrids) will still account for 90 % of total light duty vehicle powertrains in 2030 [2]. There is now a plethora of different gasoline engine technologies that are in use to reduce fuel consumption and CO_2 emissions. These include gasoline direct injection (GDI), downsizing and turbocharging, variable valve timing (VVT), cylinder deactivation (CDA), lean burn, homogeneous charge compression ignition (HCCI) and water injection [1,3,4].

Cylinder deactivation (CDA) has received attention for its ability to increase engine efficiency at part load conditions where brake specific fuel consumption (BSFC) is higher than unthrottled operation [5]. This increase in efficiency will reduce the CO_2 footprint, which is vital when looking to meet CO_2 targets. The application of CDA to part load operation offers significant potential benefits since most GDI operation is throttled [6]. This is particularly important in urban areas where the engine will operate at points of lower load. CDA functions to deactivate one or more of the engine's cylinders. This allows the cylinders that remain in operation to operate at a higher load and, therefore, more efficiently due to reduced engine throttling and pumping losses [7]. CDA works by deactivating the valves for the deactivated cylinder(s) and then cutting the fuelling. Once the higher load is required of the engine again, i.e., accelerating onto a motorway, the deactivated cylinder(s) are then restarted to provide the driver's demands.

There are studies that have quantified the fuel economy and CO_2 benefits of CDA [8] and have reported fuel saving benefits of between 9 % [9] and 16 % [10]. All of these studies evaluated the performance of CDA with the engine at part load conditions with Parker et al., Lee et al. and Kuruppu et al., all studying loads of 30 Nm [8], 32 Nm [9] and 30 Nm [10], respectively. The speed ranges tested were between 1000 rpm and 1600 rpm. It is essential to understand the engine point where the benefit was observed, as when the engine is running at a higher load, there is a reduced benefit from deactivating any cylinders.

Cylinder deactivation directly affects the engine-out emissions and

* Corresponding author.
E-mail address: g.brinklow@bham.ac.uk (G. Brinklow).

https://doi.org/10.1016/j.ceja.2023.100481

Available online 17 March 2023

exhaust gas temperatures. This will therefore have a considerable impact on the performance of the aftertreatment system – particularly the three-way catalyst (TWC). The performance of the TWC is key for vehicles passing emission regulations and improving air quality. For the TWC to perform at optimum, it requires sufficient temperatures (approx. $> 250\ ^{\circ}C$) and an exhaust gas mixture close to a lambda value of 1 or slightly rich of stoichiometric. Whilst there have been multiple studies on the fuel saving potential of CDA, there has been very limited research on the effects this has on engine-out emissions and temperatures. Parker et al. found a reduction in the CO and HC emissions of 54 % and 43 %, respectively, when running at the same operating point but with a cylinder deactivated [8]. However, there was a 30 % increase in the NO_X emissions [8]. This was related to the higher combustion temperature as the indicated mean effective pressure (IMEP) was higher for each of the firing cylinders. In addition to this, the air-fuel ratio (AFR) was leaner during the CDA operating mode [8]. Whilst the results were presented by Parker et al. for engine-out emissions, there was no report on the impact this would have on a TWC and/or tailpipe emissions. Luo et al. did study the effects of dynamic skip fire on the TWC light-off time [11]. Dynamic skip fire (DSF) is another version of the CDA technology. Lue et al. found DSF to reduce TWC light-off time by 10 %, therefore, having a positive impact on the cumulative emissions during an engine start.

The aim of this work is to provide an understanding of a CDA strategy whereby the valves remain operational whilst the cylinder is deactivated. This technology is more cost-effective than other systems reported in the literature that contain additional hardware to switch the valve actuation on and off. Investigating the effects of this CDA technology on catalyst temperature and emissions during steady state conditions will allow for a greater understanding of how CDA affects TWC performance both in terms of conversion efficiency and temperature. There is currently a gap in the literature on the interactions between the catalyst and the engine during periods of cylinder deactivation. This provides an opportunity to identify potential synergies between the engine and TWC in order to improve catalyst performance. The significance of the work is in assisting future powertrains to meet ever more stringent emission regulations.

2. Experimental

The testing was carried out at The University of Birmingham Engine Test Laboratory using a modern 3-cylinder 1.5 l turbocharged GDI engine. This engine was a contemporary EURO VI engine and featured multiple friction reducing and lightweight solutions. The TWC used for this work was selected to be representative of a typical automotive TWC. The diameter and length were 118.4 mm and 109 mm respectively. The cell density was 600 cpsi and wall thickness was 2 mil. PGM loading was 30 g/ft^3 with a ratio of 23:7 palladium to rhodium. Before the experimental work, the catalyst was aged at 1100°C in a static furnace for 10 hours.

One of the three cylinders was deactivated by cutting off the fuel to that cylinder whilst the brake torque from the engine was maintained. This caused the two active cylinders to operate at a higher load – as shown by the indicated mean effective pressure (IMEP). To achieve the same engine brake torque, the IMEP per cylinder increased from 1.2 bar to 2.4 bar during the CDA period. The valves to the cylinder operating in CDA mode were not deactivated. This led to air passing through the cylinder and towards the TWC. This increased the amount of oxygen the catalyst was exposed to depending upon the lambda control. For open-loop lambda control, the catalyst was exposed to lean conditions. This was because the fuelling was not adjusted during open-loop control. During closed-loop control, the lambda reading was fed back to the ECU, which then adjusted the fuelling to maintain lambda 1 at the exhaust (upstream from the TWC). As the air passing through the deactivated cylinder would make the exhaust gas lean, the ECU increased the fuelling to the firing cylinders to achieve lambda 1 at the exhaust.

The duration of each fuel cut was also adjusted in order to investigate the effect on the catalyst. Each test was completed at steady state conditions at an engine speed of 2000 rpm and a load of 30 Nm. This part load condition was selected as it is typical of urban vehicle operation where CDA benefits have been observed previously [12]. The experimental conditions are shown in Table 1 both for the open-loop and closed-loop lambda for each fuel cut duration.

Downstream of the engine, a close coupled TWC was mounted and then instrumented with k-type thermocouples to measure the inlet and outlet gas temperatures. In addition to this, a thermocouple was placed in contact with the inlet face to the catalyst at the axial centre to give an indication of the brick temperature. A UEGO sensor was placed before the TWC in order to understand how CDA periods affected the total engine-out lambda. Emissions before and after the TWC were measured with an MKS multigas FTIR emissions analyser and a V&F EIMS-HSense hydrogen analyser. A full schematic of the test set up is shown in Fig. 1.

3. Results and Discussions

3.1. Effect of cylinder deactivation strategies on lambda and catalyst temperature

Understanding the lambda control for the different CDA strategies will help explain the effects on the catalyst that are reported here. There are two lambda values discussed. These are exhaust lambda and combustion lambda. The exhaust lambda is the total lambda for the engine and was measured using a UEGO sensor before the TWC accounting for all 3 cylinders whether they were firing or not. The combustion lambda is the lambda value calculated by the ECU and was for the firing cylinders only. For the open-loop and closed-loop cases, the exhaust lambda values are shown in Fig. 2 for different CDA periods.

The combustion lambda was not adjusted for the open-loop CDA mode and therefore remained at 0.9985. This caused the exhaust lambda to increase from 1 to around 1.4 (as shown in Fig. 2) due to the air pumped by the deactivated cylinder. This occurred for all cases apart from the 1 second CDA test that reached a maximum lambda of 1.3. Once the CDA period ended, the exhaust lambda returned to 1 (0.9985) as all cylinders were firing again; therefore, combustion lambda was approximately the same as exhaust lambda.

The closed-loop lambda CDA operation differed from the open-loop by adjusting the combustion lambda in order to maintain an exhaust lambda of 1. During conventional operation, the exhaust lambda was 1 (0.9985). However, once the injector was deactivated in cylinder 1 the air that was pumped through the cylinder led to a lean spike in exhaust lambda which was seen at 120 seconds. The ECU reacted to this lean spike by enriching the combustion lambda to 0.7943 ± 0.004. This maintained the exhaust lambda at 1 for the duration of the CDA period. There was a rich spike when the cylinder was reactivated after the end of the CDA period. This was because combustion lambda was still rich, and the ECU needed to adjust this once all cylinders were firing again. The effect of the open-loop and closed-loop lambda control on catalyst temperature was linked to the exhaust lambda and was also of interest and is shown in Fig. 3.

Table 1
Testing plan.

Experiment	Lambda Control	CDA Duration / s	Cycles Deactivated
1a	Open-loop	60	1000
1b	Open-loop	30	500
1c	Open-loop	15	250
1d	Open-loop	5	83.33
1e	Open-loop	1	16.67
2a	Closed-loop	60	1000
2b	Closed-loop	30	500
2c	Closed-loop	15	250
2d	Closed-loop	5	83.33
2e	Closed-loop	1	16.67

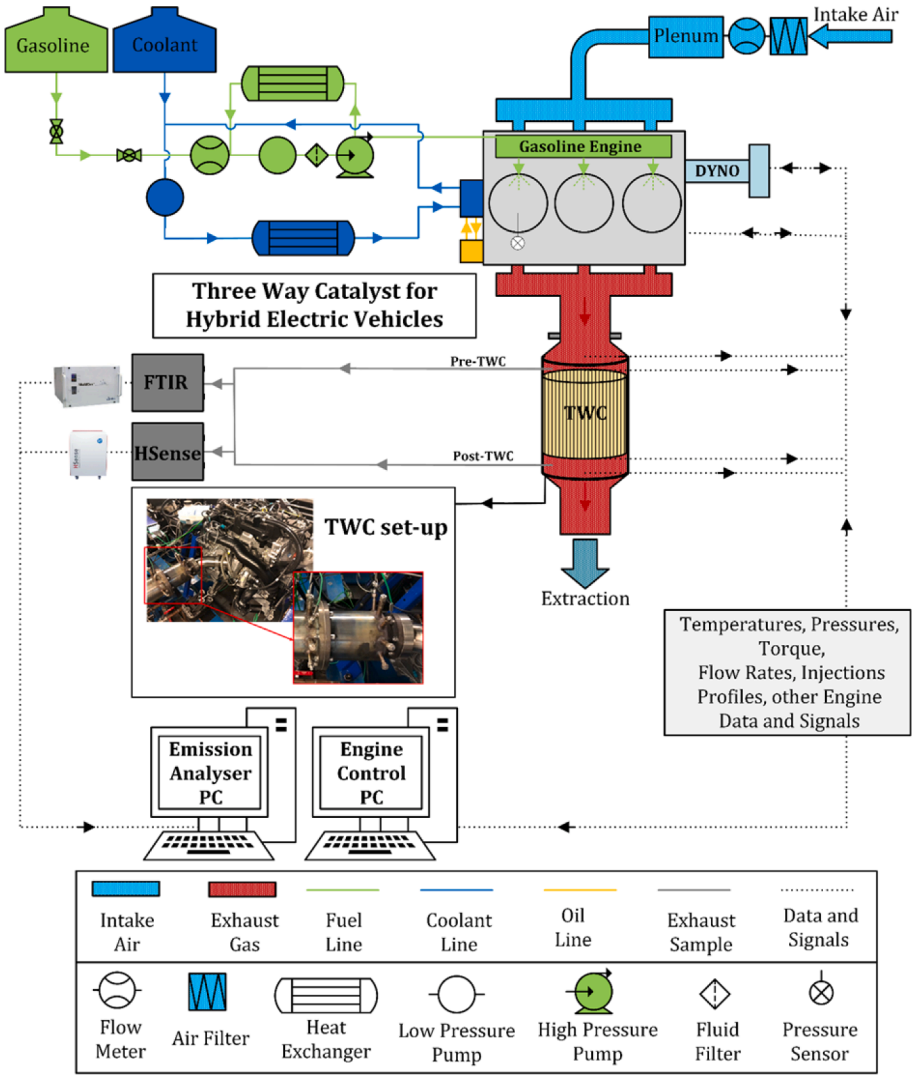

Fig. 1. Test set up schematic.

During these tests, the catalyst remained active for the whole duration of the experiment as the temperature did not drop below the catalyst light-off. Open-loop control CDA durations of less than 5 seconds provided an increase of 20°C. However, for open-loop CDA durations longer than 5 seconds, there was a drop in catalyst temperature after the initial spike. It was clear that the reduction in temperature witnessed after the first 5 seconds of CDA operation resulted from the gas temperature before the catalyst reducing by 50°C. This was because the cold air from the deactivated cylinder mixed with the combustion gases to reduce the exhaust temperature. For the initial temperature increase witnessed over the first few seconds for each open-loop lambda control test this could be a result of the switch to lean conditions. It has been reported that lean operation can increase catalyst temperature due to an exothermic reaction that occurs on the catalyst as oxygen is adsorbed onto the ceria [13]. The rise in catalyst temperature could also result from the lean exhaust gases oxidising any CO, HCs or H_2 present, however increases in temperature due to oxidation are reportedly much higher than temperature increases that result from the storage of oxygen on the ceria (which are between 15°C to 30°C) [14]. This could explain the relatively small increase in catalyst temperature and why it only occurred for a short duration as no further oxygen can be adsorbed once the oxygen storage capacity (OSC) is full. It was reported by Tsinoglou et al. that by increasing the OSC it was possible to increase the temperature increase resulting from the increase in oxidation state of the ceria [15]. This open-loop CDA operation could be applied as a catalyst heating strategy. It should be applied during catalyst warm up and once the catalyst has already reached a temperature where the ceria could adsorb the excess oxygen (approx. 150°C) [16]. For this to be successful – based on this experimental set up – the CDA period should be less than 5 seconds and occur frequently. In addition to this, the duration between CDA periods should be sufficient to allow for some of the OSC to be used.

During closed-loop CDA operation, the temperature of the catalyst increased substantially for longer periods of CDA operation. For durations of 5 seconds or less, the increase was modest with a 50°C increase for 5 seconds of closed-loop CDA. However, for 15 seconds, the catalyst temperature increased by 150°C. For the 60 second closed-loop CDA duration, the temperature increased by nearly 300°C. The increase in temperature was due to the excess CO, HCs and H_2 from the rich firing cylinders mixing with the oxygen pumped from the deactivated cylinder and reacting on the catalyst. This resulted in a large amount of heat released. There is a delay in the temperature increase from the start of the closed-loop CDA event of 20 seconds. Further study is needed to understand the reasons for this delay but there are theories as to why. The first of these is the thermal inertia of the catalyst. This is also demonstrated by the time taken for the catalyst to cool after the closed-loop CDA period has ended. Additionally, it could be related to the time taken for the reaction rate to increase. As the exotherm begins to take place reaction rates increase as the temperature increases.

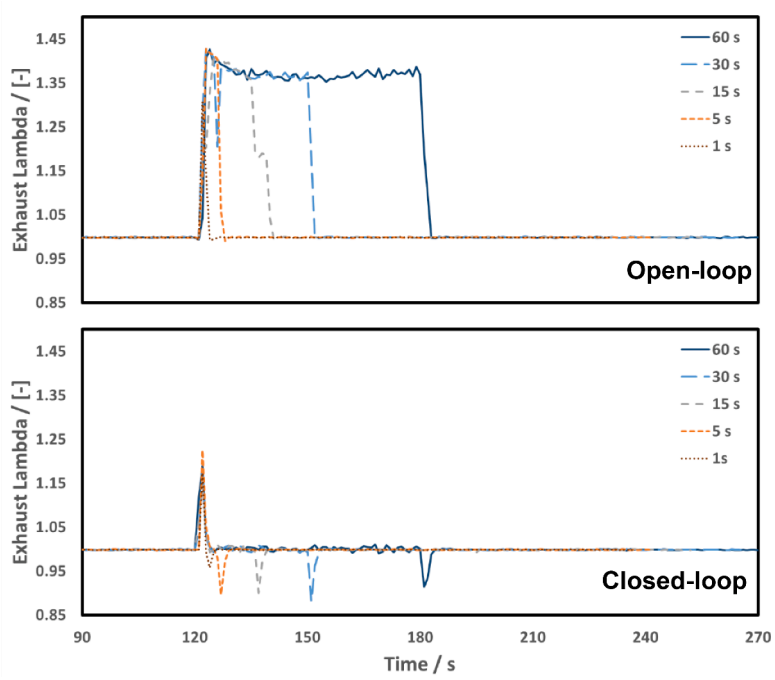

Fig. 2. Exhaust lambda for open-loop and closed-loop lambda control CDA of different durations. CDA event began at 120 seconds.

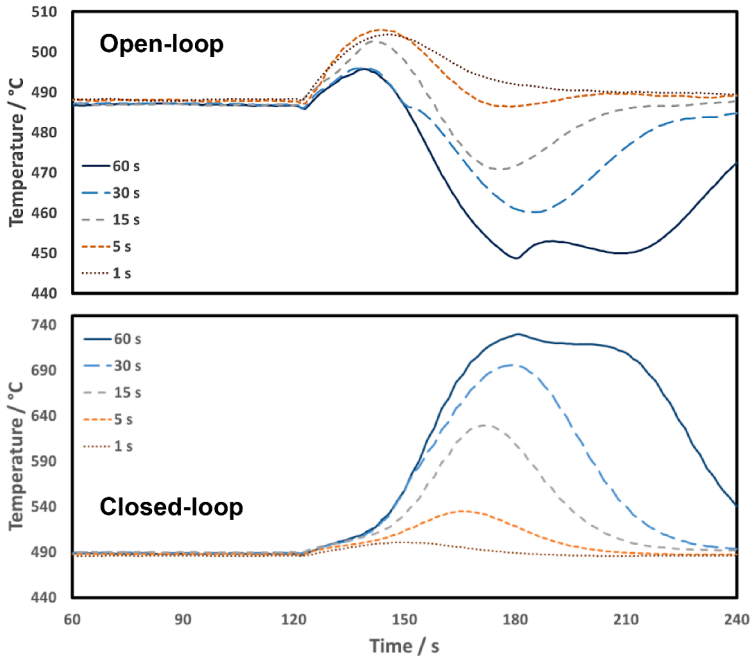

Fig. 3. TWC monolith temperature for open-loop and closed-loop lambda control CDA of different durations. CDA event began at 120 seconds. TWC temperature measurement was taken on the inlet face of the catalyst at the axial centre.

The catalyst needed to have some level of activity to start the reaction to release the heat. However, as with the open-loop CDA strategy, there is potential to reduce light-off time. Closed-loop CDA could be activated whilst the catalyst is below light-off temperature but still has some activity, and then this strategy would provide substantial heat to the catalyst and achieve light-off. It is worth noting here that there will be a reduction in the engine thermal efficiency due to the heat being released over the catalyst not being transferred to useful work during the expansion stroke in the engine cycle. For a closed-loop CDA period of 15 seconds, the total increased fuel mass was 2.15 g. When comparing this to the total fuel mass increase of ignition retard and an electrically heated catalyst, these were 5.5 g and 6.1 g, respectively, for a reduction in light-off time of 50 seconds [17].

3.2. *CO emissions*

The two main factors that will govern the mass flow rates of any emissions are the total exhaust mass flow rate and the species concentration. The total exhaust mass flow rate is controlled by the throttle and fuelling; however, the throttle has the largest effect. During the CDA

period, the engine throttle was increased to provide the additional torque required. This increased the total exhaust mass flow rate for both CDA periods by approximately 30 %. The concentration of CO before the catalyst will be affected by the combustion efficiency. If combustion is 100 % efficient i.e., all fuel is converted to CO_2 and H_2O, there will be no CO emissions. However, this is not the case and less efficient combustion will generate more CO emissions. For the concentration of CO after the catalyst it depends upon the conversion efficiency of the catalyst which is affected by temperature and exhaust lambda. The mass flow rate of CO measured before and after the catalyst during open-loop CDA operation is plotted in Fig. 4.

During the open-loop CDA period, there was an increase in the CO mass flow rate before the catalyst from 0.2 kg/hr to 0.23 kg/hr. This represented an increase in mass flow of 15 %. Since this increase was lower than the total exhaust mass flow rate increase (30 %) it represented a relative reduction in CO compared to other species. This was true with the CO concentration reducing from 6,300 ppm to 5,000 ppm. This indicated that combustion efficiency was increased as more carbon within the fuel was being fully oxidised to CO_2. This also matched the brake thermal efficiency, which increased from 25 % to 26 %.

The mass flow rate of CO after the catalyst was already low due to the high conversion over the catalyst (≈ 95 %). This was further improved with open-loop CDA as the conversion efficiency reached 100 %. This improvement resulted from the increase in available oxygen before the catalyst (Fig. 2).

Due to the lean conditions during the open-loop CDA period a large amount of oxygen was provided to the catalyst filling its OSC. The theoretical maximum OSC of the catalyst was estimated from the catalyst dimensions and CeZr loading by using the method described in [18] to be 1,531 mg of O. It was then calculated following the equation published in [19] that operating in the open-loop CDA mode would fill the theoretical maximum OSC in 2.12 seconds. Since the catalyst was aged, the actual OSC of the storage would be less. With this consideration it can be claimed that operating for 1 second in the open-loop CDA mode would if not completely, very nearly fill the available OSC. Once the cylinder was reactivated and the exhaust lambda returned to approximately 1 (0.9985), there was a period of over a minute until the CO mass flow rate after the catalyst began to increase. Assuming a full OSC on a fresh catalyst it was estimated that the OSC could provide 264 seconds of oxygen buffer before the CO emissions would increase again. Since an aged catalyst was used for this work, the observed buffer time of ≈ 150 s (Fig. 4) is expected due to the aging of the OSC. This additional oxygen storage could be useful for helping the catalyst manage richer spikes in engine-out emissions such as during acceleration events.

The mass flow rate of CO emissions before and after the catalyst during the closed-loop CDA tests is shown in Fig. 5. The engine-out mass flow rate of CO during the closed-loop CDA period increased from 0.2 kg/hr to up to 1.8 kg/hr. This increase was 8 times larger than the increase in the overall exhaust mass flow rate, indicating an increase in CO emissions from the engine which was seen by an increase in CO concentration from 6,300 ppm to 35,000 ppm. This indicated reduced combustion efficiency since only partial oxidation was able to take place due to the lack of available oxygen with a combustion lambda of 0.8.

The mass flow rate of CO after the catalyst was relatively low, with the catalyst having a conversion efficiency of ≈ 96 %. However, during the closed-loop CDA operation, the mass flow rate of CO was reduced to 0 kg/hr. This high CO conversion of the catalyst was obtained despite the high CO mass flow rate before the catalyst during the closed-loop CDA period. This high mass of CO being oxidised will – if all CO is oxidised – generate approximately 4.7 kW of heat. Transferring this amount of heat to the catalyst would explain some of the temperature increases witnessed in Fig. 3.

The oxygen supplied to the catalyst during the closed-loop CDA period was sufficient to oxidise all the CO and fill some of the OSC. This was similar to the open-loop CDA case. However, the OSC was not completely filled due to the oxygen demand due to the increased CO and HC species. Therefore, the period of improved CO conversion after the end of the CDA period was shortened.

3.3. Hydrocarbon emissions

The effect of CDA strategy on HC emissions is essential due to the harmful and carcinogenic effects of certain HC species to the human body and the harmful effects on the environment of some HC species [20,21]. Additionally, emission regulations limit the total hydrocarbon emissions from vehicles. The HC mass flow rate before and after the

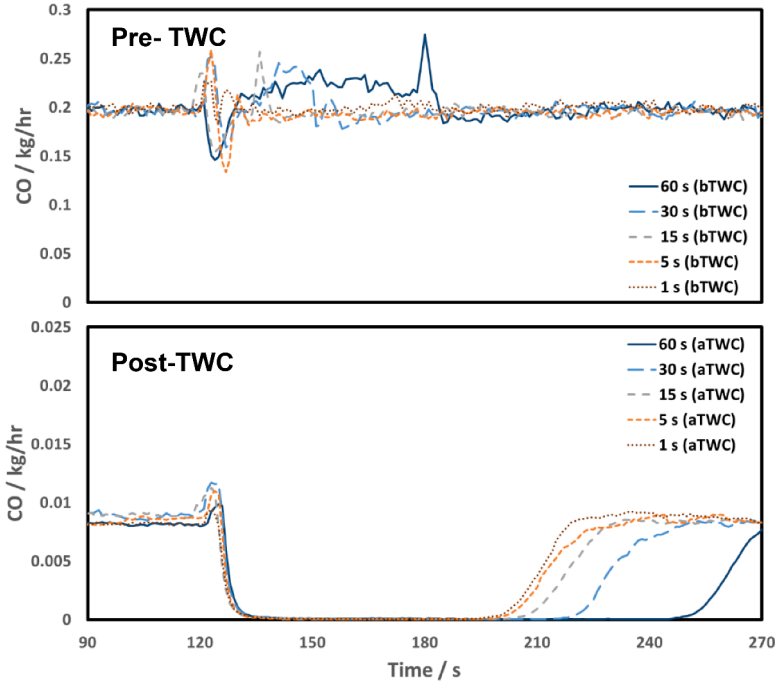

Fig. 4. CO mass flow rate for open-loop lambda control CDA of different durations. CDA event began at 120 seconds.

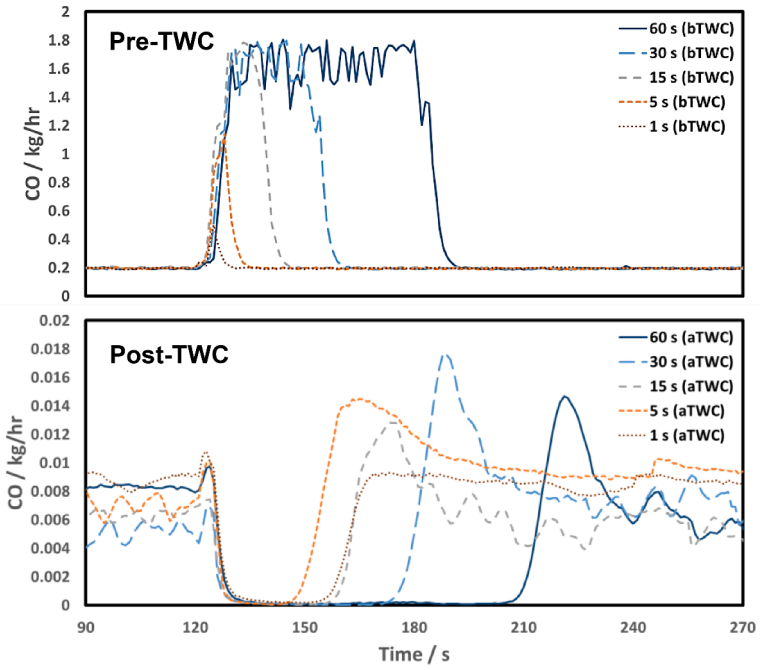

Fig. 5. CO mass flow rate for closed-loop lambda control CDA of different durations. CDA event began at 120 seconds.

catalyst during the open-loop CDA was similar to the baseline engine condition and therefore is not shown in the interests of brevity. The causes for the similar mass flow rates before the catalyst was the trade-off between the increased mass flow rate and the reduced HC concentration. The HC concentration before the catalyst reduced from 2, 400 ppm to 1,700 ppm which supports the increase in brake thermal efficiency due to more efficient combustion. These results suggest there to be little effect on catalyst HC performance during open-loop CDA.

The HC mass flow rate before and after the catalyst is shown in Fig. 6 for the closed-loop CDA operating mode. The closed-loop CDA mode doubled the engine-out HC mass flow rate. This increase further supports the effect of closed-loop CDA on combustion efficiency. The richer combustion resulted in increased HC emissions since there was insufficient oxygen available in the cylinder to completely oxidise all HCs. Any HC species that are present in the exhaust have not been used to produce any useful work during the engine expansion/power stroke, so this represented a loss in engine efficiency.

The mass flow rate of HCs after the catalyst was characterised by a peak when the engine first switched to the closed-loop CDA operating mode. This peak coincided with the increase in HC mass flow rate before the catalyst. Upon further analysis of the hydrocarbon species, it was found that methane slip was the contributor to this. However, the catalyst was able to still maintain a relatively high conversion efficiency of ≈ 90 % even during this transition period. This high amount of HC

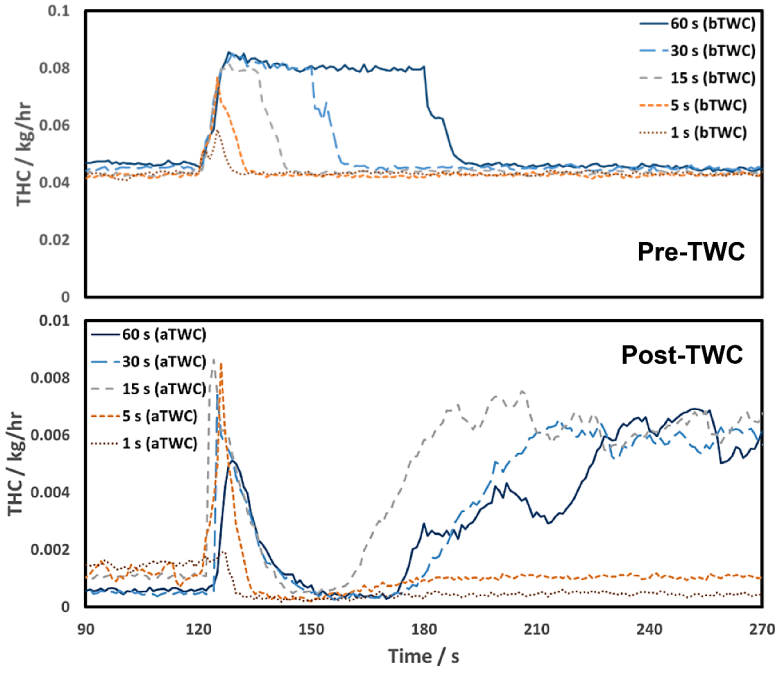

Fig. 6. THC mass flow rate for closed-loop lambda control CDA of different durations. CDA event began at 120 seconds.

oxidation over the catalyst caused – along with the CO oxidation – the large temperature exotherm witnessed during the closed-loop CDA operation. After the transition period, the HC mass flow rate after the catalyst was essentially 0 kg/hr. This was despite the increase in HCs before the catalyst. The oxygen provided by the deactivated cylinder was sufficient to help oxidise the HC species over the catalyst but only for a limited duration. With closed-loop CDA durations of 15 seconds or longer, there was an increase in HC mass flow rate after the CDA period. By assessing the individual hydrocarbon species, it was observed that this post CDA increase resulted from propane slip. This could be a result of the increased HC concentration before the catalyst. However, during the closed-loop CDA period the exhaust lambda was slightly lean (1.0006) which suggests that it was not a result of the OSC being depleted. An alternative cause could be due to the large amount of HC species before the catalyst during the closed-loop CDA operation. Catalyst performance can be inhibited if some of these species were adsorbed onto the surface, although at the temperatures recorded during this period it is unlikely. A more likely cause could be the deposition of coke onto the Pd particles that cover the active surface [22]. Until this is cleared, and the adsorption sites became available again, conversion will suffer. This is also supported by the fact that the increase in HC emissions was due to short chain saturated species with high diffusivity [23]. This competition between species for active site availability could be linked to the increase in HC emissions post catalyst.

3.4. Nitric oxide emissions

Nitric oxide is a regulated pollutant; therefore, vehicles must ensure they keep NO emissions below the regulated threshold. NO is of concern due to its ability to rapidly oxidise to NO_2 in the atmosphere, which contributes to smog and acid rain. Furthermore, NO_2 is harmful to the human respiratory system [24]. The mass flow rate of NO before and after the catalyst during the open-loop CDA period is shown in Fig. 7.

The engine-out NO mass flow rate increased during the open-loop CDA period by approximately 37.5 %. The cause for this was not only the increase in exhaust mass flow rate but the increased load of the two firing cylinders. The increase in IMEP for each cylinder led to higher combustion temperatures and, therefore an increase in NO formation via the Zeldovich mechanism [25]. Since the increase in NO mass flow rate was higher than the increase in total mass flow rate it suggests that the increase in NO mass flow rate was a result of the higher IMEP for the two firing cylinders.

The NO mass flow rate after the catalyst during the baseline operation was 0 kg/hr with the catalyst operating at a conversion efficiency of 100 %. However, during the open-loop CDA operating mode there was a breakthrough of NO after the catalyst. This was a result of both the increase in NO mass flow rate before the catalyst and the increase in lambda. The increase in lambda due to the oxygen provided by the air pumped by the deactivated cylinder will reduce NO conversion in the catalyst. There was still some conversion of approximately 10 % but the catalyst did not reduce the majority of NO. For the shorter open-loop CDA durations, there was a less pronounced increase in the mass flow rate of NO post catalyst. Durations of open-loop CDA lasting less than 5 seconds could provide benefits without the penalty of NO slip. This contrasts with the improvement in CO conversion, which lasted 60 seconds after the CDA period. The duration of open-loop CDA operation before NO slip occurs will depend upon the state of the OSC before the CDA operation, total catalyst OSC (also a function of catalyst age) and the number of cylinders deactivated.

The mass flow rate before and after the catalyst for the closed-loop CDA operation mode is plotted in Fig. 8 for each duration of CDA tested. The mass flow rate of NO before the catalyst reduced significantly during the closed-loop CDA period. This was despite the increase in overall exhaust mass flow rate during the CDA period. The reduction in NO resulted from the rich combustion taking place in the two firing cylinders ($\lambda \approx 0.8$). This provided little to no additional oxygen that could have been used in order to react with the nitrogen in the air. It is worth noting that there was a lag of roughly 4 seconds between the deactivation of the cylinder and the engine increasing the fuelling to the firing cylinders to achieve a total exhaust lambda of 1. During this time, the IMEP of the individual firing cylinders was increasing, which led to the initial spike in NO witnessed when the engine first switched to the closed-loop CDA mode. Then as the fuelling was increased to balance the lambda, the NO production in the engine dropped.

The mass flow rate of NO after the catalyst increased during the closed-loop cylinder deactivation period. During the baseline operation, the NO conversion efficiency was 100 %. However, during the closed-loop CDA period, the NO conversion efficiency dropped to 0 % as all

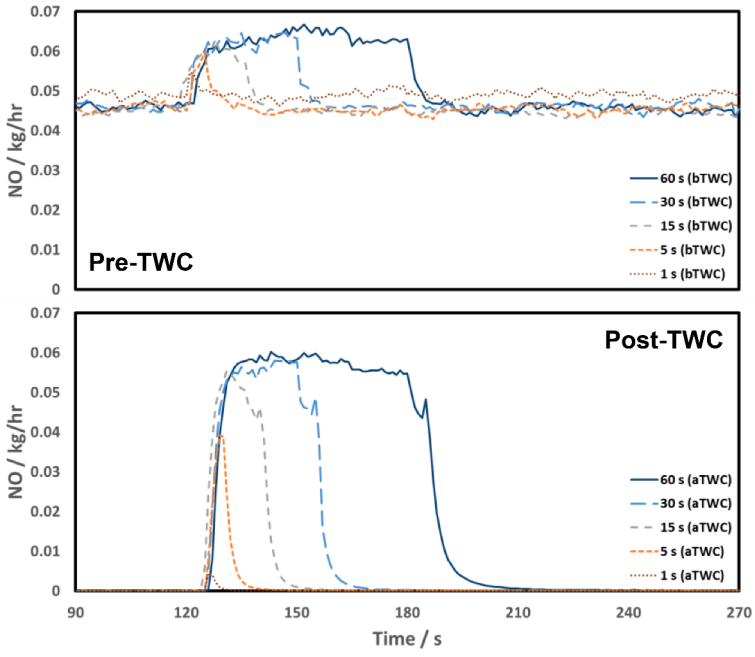

Fig. 7. NO mass flow rate for open-loop lambda control CDA of different durations. CDA event began at 120 seconds.

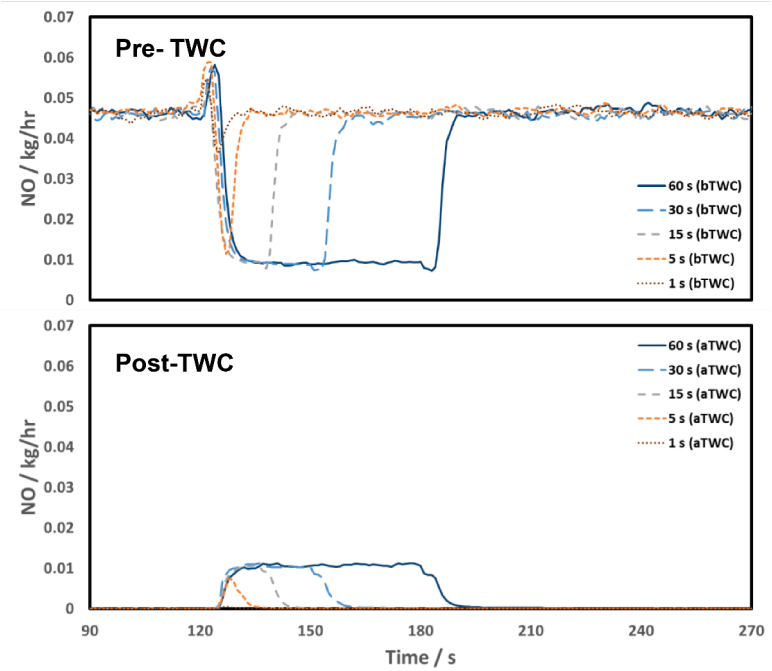

Fig. 8. NO mass flow rate for closed-loop lambda control CDA of different durations. CDA event began at 120 seconds.

NO produced by combustion was passed straight through the catalyst. This was true for closed-loop CDA periods of 5 seconds or greater. For the 1 second CDA period, there was no loss in NO catalyst activity as it was able to use the OSC as a buffer. This contrasted to the 1 second open-loop CDA where there was NO slip. This difference between the NO emissions was a result of the different exhaust lambdas. Due to the stoichiometric conditions for the catalyst during the closed-loop CDA mode, the OSC could reduce the NO for a limited duration until it is full. Despite the reduction in engine-out NO and the stoichiometric exhaust gas during the closed-loop cylinder deactivation, the catalyst was unable to reduce the NO. This could result from the increased demand placed upon the catalyst active sites by the increased levels of CO and HCs.

3.5. Nitrogen dioxide emissions

The mass flow rate of NO_2 before and after the catalyst is shown in Fig. 9 for each open-loop CDA operation period.

The mass flow rate of NO_2 out of the engine was 0 kg/hr during conventional engine operation. This was because the formation of NO_2 requires an excess of oxygen which was not present during stoichiometric combustion. However, once the open-loop cylinder deactivation period began, there was an increase in the engine-out NO_2 mass flow rate. This increase was tied to the increased NO emissions that were produced by the higher combustion temperatures during the open-loop CDA operation. Once the NO emissions in the exhaust gas from the two

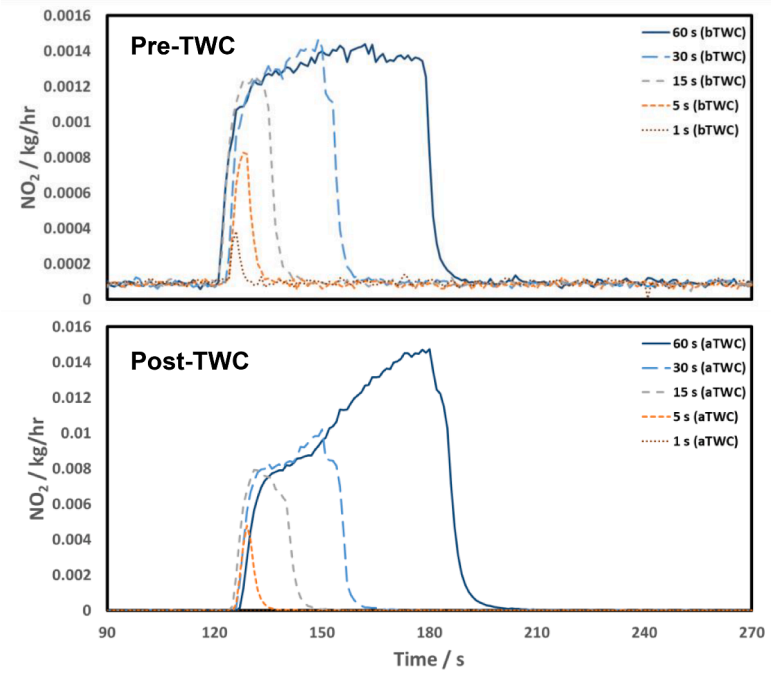

Fig. 9. NO_2 mass flow rate for open-loop lambda control CDA of different durations. CDA event began at 120 seconds.

firing cylinders mixed with the oxygen provided by the air pumped by the deactivated cylinder there was oxidation of some of the NO into NO_2. However, the NO_2 mass flow rate was still very low, with a NO to NO_2 ratio of 70 during the open-loop cylinder deactivation period.

The mass flow rate of NO_2 after the catalyst increased during the open-loop CDA period. NO_2 was produced as a secondary emission over the catalyst during the open-loop cylinder deactivation. As the duration of open-loop CDA continued, the NO_2 mass flow rate continued to increase. This could be as more oxygen became available. The catalyst did increase oxidation of NO into NO_2. If the CDA duration was around 1 second, then there were no NO_2 emissions recorded after the catalyst. This suggests that there was enough empty OSC on the catalyst during this initial second to reduce the NO and prevent formation of NO_2. It also explains the increased production of NO_2 over the catalyst as the OSC was filled during the longer open-loop CDA periods.

The NO_2 mass flow rate before and after the catalyst is shown in Fig. 10 for the closed-loop CDA period. The mass flow rate of NO_2 from the engine was essentially zero during the baseline operation due to the lack of additional oxygen for the combustion. Once the closed-loop CDA period began, the engine-out mass flow rate of NO_2 increased. The increase was caused by the NO from the two firing cylinders mixing with the oxygen from the air of the deactivated cylinder. However, the increase was not as great as the increase during the open-loop cylinder deactivation period. This was due to two factors. The first of these was the lower production of NO within the firing cylinders, as the combustion was richer during the closed-loop cylinder deactivation period. The second of these was the overall richer exhaust gas meaning that the excess CO and HCs within the exhaust consumed oxygen instead of there being a large excess to oxidise the NO.

The mass flow rate of NO_2 after the catalyst showed a different trend during the closed-loop CDA. The first difference was that the mass flow rate of NO_2 after the catalyst was lower than the mass flow rate of NO_2 before the catalyst. This showed that there was conversion of NO_2 over the catalyst. This conversion was due to the exhaust lambda remaining stoichiometric during the closed-loop CDA operation. This created an environment that allowed for increased NO_2 reduction. The other difference was that the NO_2 mass flow rate after the catalyst continued to decrease during the 60 second CDA period. This suggests the environment for the catalyst during the closed-loop CDA period was sufficiently reducing to prevent NO_2 emission. The spike in NO_2 emissions could be the result of the lean spike seen when the engine changes from the baseline condition to the closed-loop CDA condition (Fig. 2). However, as the fuelling was adjusted to maintain the exhaust lambda at a value of 1, the NO_2 emissions after the catalyst reduced.

3.6. Ammonia and nitrous oxide emissions

NH_3 and N_2O are key currently unregulated emission species. Both species are secondary emissions that are formed within the TWC at certain operating conditions. N_2O is a greenhouse gas with a global warming potential that is 300 times that of CO_2 whilst NH_3 contributes to particulate matter through secondary aerosol formation [26,27]. There was no N_2O formation over the catalyst since N_2O is formed at lower catalyst temperatures which were not investigated during these experiments. However, NH_3 formation over the catalyst does take place at typical catalyst operating temperatures [28]. There was no production of NH_3 during combustion as expected. This was indicated by the engine-out NH_3 mass flow rate that was essentially 0 kg/hr. In the interest of brevity, the engine out NH_3 mass flow rate is not presented here. The mass flow rate of NH_3 after the catalyst is shown in Fig. 11 for all durations of the open-loop and closed-loop CDA operation.

The mass flow rate of NH_3 after the catalyst showed there to be production of NH_3 during the baseline engine operation. This was expected since the engine lambda was slightly rich at 0.9985. When there is insufficient oxygen, NO can be oxidised by CO, H_2 or HC species, leading to the formation of NH_3 [29]. However, once the open-loop CDA operating mode was activated, there was a drop in the NH_3 production over the catalyst. This was due to the increase in exhaust lambda. After the open-loop CDA period finished, there was still a decrease in the formation of NH_3 over the catalyst. This period lasted for up to 90 seconds, even for the 1 second open-loop CDA case. This period of inhibited NH_3 formation occurred due to the filling of the OSC on the catalyst during the open-loop CDA period as discussed previously with the theoretical maximum oxygen buffer at this condition being 264 s. With the OSC on the catalyst filled, it was able to provide oxygen to inhibit NH_3 formation. Using a 1 second open-loop CDA duration could limit the

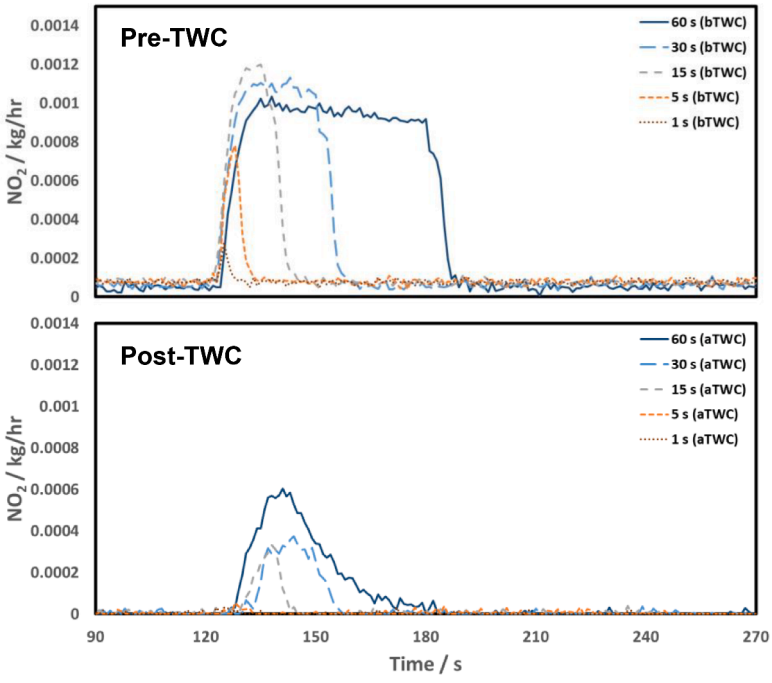

Fig. 10. NO_2 mass flow rate for closed-loop lambda control CDA of different durations. CDA event began at 120 seconds.

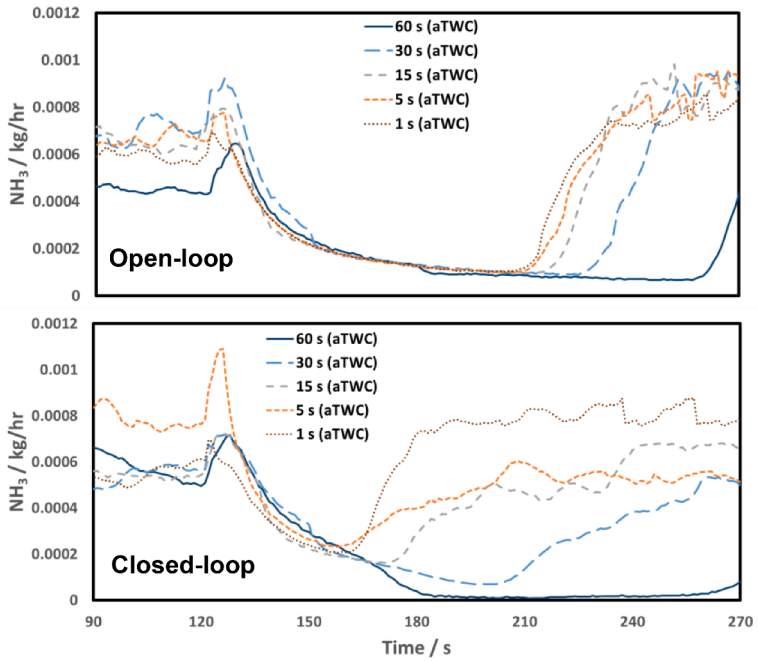

Fig. 11. NH_3 mass flow rate for open-loop and closed-loop lambda control CDA of different durations. CDA event began at 120 seconds.

formation of NH_3 in addition to improving CO conversion whilst incurring a minimal NO_X penalty.

For the closed-loop CDA period the mass flow rate of NH_3 before the catalyst was again 0 kg/hr indicating that there was no formation of NH_3 during combustion. However, there was a small increase during the closed-loop CDA period. This was most likely some of the NO reacting with the H_2 or HCs that were present in large quantities in the rich combustion gases. Measurements of NH_3 after the catalyst indicated the same trends that were recorded for the open-loop CDA operation period. There was some difference between the two strategies as the period of reduced NH_3 formation was shorter than the one that resulted from the open-loop CDA period. This was because the OSC was not filled as much as it was during the open-loop CDA period. If NH_3 production over the catalyst is of concern it would be recommended to operate with a short and occasional open-loop cylinder deactivation period.

4. Conclusions

The open-loop CDA operation mode was able to improve CO conversion and prevent NH_3 formation over the catalyst. This was achievable with just 1 second of open-loop CDA operation with the benefit lasting for approximately 60 and 90 seconds for the CO and NH_3 performance respectively. The drawback of increased NO_X became an issue with increased time spent in the open-loop CDA mode. However, once the CDA period had finished, the NO_X breakthrough post catalyst stopped immediately. This suggests that for short periods of open-loop CDA operation catalyst CO and NH_3 performance can be improved with little to no NO_X penalty. Furthermore, operating the engine in open-loop CDA mode was able to improve engine efficiency and reduce fuel consumption.

The main benefit observed during the closed-loop CDA period was the increase in catalyst temperature. This could be used as an effective catalyst heating strategy that would assist in reducing light-off time and therefore emissions. This would be particularly useful for engines integrated into PHEVs and HEVs where the engine will start and stop multiple times over a single journey at a variety of different catalyst temperatures. The increase in fuel consumption related to the catalyst heating was lower than the increases associated with retarded ignition timing and electrically heated catalysts. The increase in post catalyst NO_X emissions can be addressed by applying shorter durations of closed-loop CDA operation.

Further work is recommended to investigate how the optimisation of CDA strategies can improve the exhaust aftertreatment performance to abate regulated and non-regulated emissions under real driving emission conditions in conventional and electrified vehicles. Comparison of CDA strategies in terms of catalyst light-off time reduction and energy/equivalent fuel usage should be made to other catalyst heating strategies such as secondary air injection, exhaust burners, or electrically heated catalysts.

CRediT authorship contribution statement

George Brinklow: Conceptualisation, experimental work, data analysis, writing. **Jose Martin Herreros**: Conceptualisation, data analysis, review and editing, supervising, funding acquisition. **Soheil Zeraati Rezaei**: Experimental work, data analysis, review and editing. **Omid Doustdar**: Experimental work, data analysis, review and editing. **Athanasios Tsolakis**: Review and editing, supervising, funding acquisition. **Paul Millington**: Review and editing, supervising. **Amy Kolpin**: Review and editing, supervising.

Funding Information

Funding was provided by the EPSRC in the form of a PhD student stipend and additional funding was provided by Johnson Matthey PLC in the form of laboratory consumables and test materials.

Declaration of Competing Interest

The authors declare the following financial interests/personal relationships which may be considered as potential competing interests:

Data availability

Data will be made available on request.

Supplementary materials

Supplementary material associated with this article can be found, in the online version, at doi:10.1016/j.ceja.2023.100481.

References

[1] A. Joshi, Review of Vehicle Engine Efficiency and Emissions, SAE Tech. Pap. 2020-April (April) (2020) 1–29.
[2] S. Shuai, X. Ma, Y. Li, Y. Qi, H. Xu, Recent Progress in Automotive Gasoline Direct Injection Engine Technology, Automot. Innov. 1 (2) (2018) 95–113.
[3] F. Duronio, A. De Vita, A. Montanaro, C. Villante, Gasoline direct injection engines – A review of latest technologies and trends. Part 2, Fuel 265 (July 2019) (2020), 116947.
[4] P. Wieske, et al., Optimisation of gasoline engine performance and fuel consumption through combination of technologies, MTZ Worldw 70 (11) (2009) 30–36.
[5] K. Fridrichová, L. Drápal, J. Vopařil, J. Dlugoš, Overview of the potential and limitations of cylinder deactivation, Renew. Sustain. Energy Rev. 146 (April) (2021).
[6] P. Freeland, G. Jones, R.S. Chen, L.W. Huang, M. El-Kassem, R. Kaiser, An Assessment and Comparison of De-Throttling Approaches and Technologies for Further Reductions in Fuel Consumption in a Modern GDI Engine, SAE Tech. Pap. 2017-Octob (2017).
[7] M.F. Muhamad Said, A. Bin Abdul Aziz, Z. Abdul Latiff, A. Mahmoudzadeh Andwari, S.N. Mohamed Soid, Investigation of Cylinder Deactivation (CDA) Strategies on Part Load Conditions, SAE Tech. Pap. 2014-Octob (2014).
[8] M.C. Parker, C. Jiang, D. Butcher, A. Spencer, C.P. Garner, D. Witt, Impact and observations of cylinder deactivation and reactivation in a downsized gasoline turbocharged direct injection engine, Int. J. Engine Res. 22 (4) (2021) 1367–1376.
[9] D.H. Lee, D. Kim, W.J. Jeon, Y.S. Hong, J.W. Park, Effect of a Cylinder Deactivation Actuator with Electro-Mechanical Switching System on Fuel Economy of an Automotive Engine, SAE Tech. Pap. 2020-April (April) (2020) 1–10.
[10] C. Kuruppu, A. Pesiridis, S. Rajoo, Investigation of cylinder deactivation and variable valve actuation on gasoline engine performance, SAE Tech. Pap. 1 (2014).
[11] X. Luo, S. Hashemi, R. Subramanian, A. Arvanitis, M. Younkins, Fast Catalyst Light-Off with Dynamic Skip Fire, SAE Tech. Pap. 2020-April (April) (2020) 1–13.
[12] A. Bech, P.J. Shayler, M. McGhee, The Effects of Cylinder Deactivation on the Thermal Behaviour and Performance of a Three Cylinder Spark Ignition Engine, SAE Int. J. Engines 9 (4) (2016) 1999–2009.
[13] D. Shah, K. Premchand, D. Pedro, Control Oriented Physics Based Three-Way Catalytic Converter Temperature Estimation Model for Real Time Controllers, SAE Tech. Pap. 2020-April (April) (2020) 1–9.
[14] C. Brinkmeier, C. Schön, G. Vent, C. Enderle, Catalyst temperature rise during deceleration with fuel cut, SAE Tech. Pap. 115 (2006) 144–154.
[15] D.N. Tsinoglou, G.C. Koltsakis, J.C. Peyton Jones, Oxygen storage modeling in three way catalytic converters, Ind. Eng. Chem. Res. 41 (5) (2002) 1152–1165.
[16] A.V. Porsin, E.A. Alikin, V.I. Bukhtiyarov, A low-temperature method for measuring oxygen storage capacity of ceria-containing oxides, Catal. Sci. Technol. 6 (15) (2016) 5891–5898.
[17] J.T.B.A. Kessels, D. Foster, W.A.J. Bleuanus, Fuel Penalty Comparison for (Electrically) Heated Catalyst Technology, Oil Gas Sci. Technol. 65 (1) (2010) 47–54.
[18] T. Khossusi, R. Douglas, G. McCullough, Measurement of oxygen storage capacity in automotive catalysts, Proc. Inst. Mech. Eng. Part D J. Automob. Eng. 217 (8) (2003) 727–733.
[19] B. Odendall and M. Schneider, "Method for Determining the Oxygen Storage Capacity," US 8,225,649 B2, 2012.
[20] R. Ballesteros, Á. Ramos, J. Sánchez-Valdepeñas, Particle-bound PAH emissions from a waste glycerine-derived fuel blend in a typical automotive diesel engine, J. Energy Inst. 93 (5) (2020) 1970–1977.
[21] X. Hao, X. Zhang, X. Cao, X. Shen, J. Shi, Z. Yao, Characterization and carcinogenic risk assessment of polycyclic aromatic and nitro-polycyclic aromatic hydrocarbons in exhaust emission from gasoline passenger cars using on-road measurements in Beijing, China, Sci. Total Environ. 645 (2018) 347–355.
[22] A. Fujiwara, Y. Tsurunari, S. Iwashita, H. Yoshida, J. Ohyama, M. Machida, Surface State Changes of Pd Three-Way Catalysts under Dynamic Lean/Rich Perturbation Compared with Static Condition, J. Phys. Chem. C 127 (1) (2023) 279–288.
[23] J.E. Johnson, D.B. Kittelson, Deposition, diffusion and adsorption in the diesel oxidation catalyst, Appl. Catal. B Environ. 10 (1–3) (1996) 117–137.
[24] R. Kurtenbach, J. Kleffmann, A. Niedojadlo, P. Wiesen, Primary NO2 emissions and their impact on air quality in traffic environments in Germany, Environ. Sci. Eur. 24 (6) (2012) 1–8.
[25] A. Alagumalai, A. Jodat, O. Mahian, B. Ashok, NOx formation chemical kinetics in IC engines, Elsevier Inc., 2021.
[26] S.K. Hoekman, Review of Nitrous Oxide (N2O) Emissions from Motor Vehicles, SAE Int. J. Fuels Lubr. 13 (1) (2020) 79–98.
[27] Z. Bao, et al., Effects of NH3 on secondary aerosol formation from toluene/NOx photo-oxidation in different O3 formation regimes, Atmos. Environ. 261 (February) (2021), 118603.
[28] C. Wang, et al., Ammonia Formation over Pd/Rh Three-Way Catalysts during Lean-to-Rich Fluctuations: The Effect of the Catalyst Aging, Exhaust Temperature, Lambda, and Duration in Rich Conditions, Environ. Sci. Technol. 53 (21) (2019) 12621–12628.
[29] P. Nevalainen, et al., Formation of NH3 and N2O in a modern natural gas three-way catalyst designed for heavy-duty vehicles: the effects of simulated exhaust gas composition and ageing, Appl. Catal. A Gen. 552 (December 2017) (2018) 30–37.